Optical fiber-based photocathode

Albert Căsăndruc, Robert Bücker, Günther Kassier, and R. J. Dwayne Miller

Articles you may be interested in

Ultrafast electron diffraction optimized for studying structural dynamics in thin films and monolayers
Structural Dynamics **3**, 034302 (2016); 10.1063/1.4949538

Bandgap modulation in photoexcited topological insulator Bi_2Te_3 via atomic displacements
The Journal of Chemical Physics **145**, 024504 (2016); 10.1063/1.4955188

 Molecular dynamics investigation of desorption and ion separation following picosecond infrared laser (PIRL) ablation of an ionic aqueous protein solution
The Journal of Chemical Physics **145**, 204202 (2016); 10.1063/1.4967164

Calculation of x-ray scattering patterns from nanocrystals at high x-ray intensity
Structural Dynamics **3**, 054101 (2016); 10.1063/1.4958887

Optical fiber-based photocathode

Albert Căsăndruc,[1] Robert Bücker,[1] Günther Kassier,[1] and R. J. Dwayne Miller[1,2]

[1]*Max Planck Institute for the Structure and Dynamics of Matter, Center for Free Electron Laser Science (CFEL) and Hamburg Centre for Ultrafast Imaging (CUI), Luruper Chaussee 149, Hamburg 22761, Germany*
[2]*Departments of Chemistry and Physics, University of Toronto, Toronto, Ontario M5S 3H6, Canada*

We present the design of a back-illuminated photocathode for electron diffraction experiments based on an optical fiber, and experimental characterization of emitted electron bunches. Excitation light is guided through the fiber into the experimental vacuum chamber, eliminating typical alignment difficulties between the emitter metal and the optical trigger and position instabilities, as well as providing reliable control of the laser spot size and profile. The in-vacuum fiber end is polished and coated with a 30 nm gold (Au) layer on top of 3 nm of chromium (Cr), which emits electrons by means of single-photon photoemission when femtosecond pulses in the near ultraviolet (257 nm) are fed into the fiber on the air side. The emission area can be adjusted to any value between a few nanometers (using tapered fibers) and the size of a multi-mode fiber core (100 μm or larger). In this proof-of-principle experiment, two different types of fibers were tested, with emission spot diameters of 50 μm and 100 μm, respectively. The normalized thermal electron beam emittance (TE) was measured by means of the aperture scan technique, and a TE of 4.0 π nm was measured for the smaller spot diameter. Straightforward enhancements to the concept allowed to demonstrate operation in an electric field environment of up to 7 MV/m. *Published by AIP Publishing.* [http://dx.doi.org/10.1063/1.4962147]

Ultrafast electron diffraction (UED) is a highly successful technique for structural dynamics investigation of phase transitions, electron-phonon coupling, and chemical reactions.[1–9] Metal photocathodes are currently the most commonly employed electron sources due to their robustness, ultrafast temporal response, and compatibility with high electric fields. They provide sub-picosecond electron pulses with coherence lengths up to a few nanometers. Extending this technique for tracking ultrafast structural changes within large unit cell systems like protein crystals requires maximization of beam brightness, by reducing the thermal emittance (TE) of the source, and increasing the pulse charge. One of the most straightforward ways for achieving the former is reducing the electron source size while maintaining the beam parallelism. The conventional method of focusing the triggering laser onto a large-area planar photocathode is subject to the spatial constraints of high voltage electrodes and makes these requirements difficult to achieve. Our approach evades this issue by directly coating a thin photocathode on the face of an optical fiber, through which the triggering beam is propagating (Figure 1(a)). This allows precise and stable control of emission area, beam profile, and pulse length by optimizing the parameters of the fiber itself, rather than by controlling or shaping the triggering laser beam. While the idea of using a fiber has been presented before,[10–12] these attempts used an etched fiber tip[13–15] featuring a semiconductor coating, wherein the optical triggering has been done externally, without exploiting the waveguiding of the fiber, and an optical alignment was still needed. In our previous paper,[16] we presented optically induced Schottky emission from a fiber tip. In this letter, we prove the functionality of the fiber photocathode concept in the photoemission mode, with target applications in low energy compact DC setups.

Two different types of fibers were tested here, with mode field diameters of 50 μm and 100 μm, respectively, and different material properties as discussed below. Two different experimental setups were used, the first for surface electric fields of up to 1 MV/m, and the second for fields of up to 7 MV/m. In the low electric field setup, which will be discussed first, a laser wavelength of 257 nm (4th harmonic of a Yb:KGW regenerative amplifier at 1030 nm (Light Conversion PHAROS)) was used, with a pulse duration of 170 fs at 1 kHz repetition rate. As opposed to our previous work,[16] the fiber tips are no longer tapered but cut off straight and attached to a special metallic fiber plug which is then polished and coated with a 30 nm thick Au layer on top of a 3 nm adhesion layer of Cr (Figure 1(a)). The emission area in this configuration is given by the size of the optical fiber core.
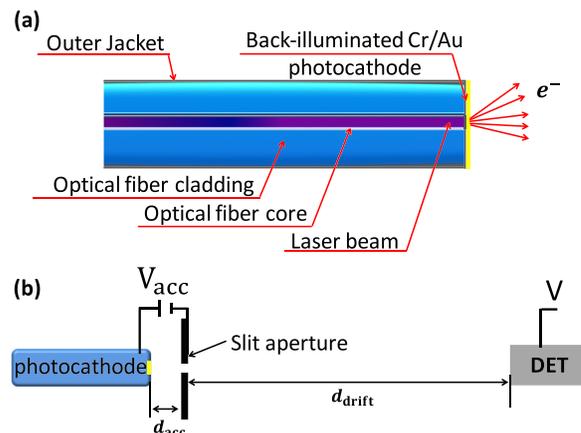
FIG. 1. (a) Sketch of the fiber-based photocathode. The emission area is equal to the core size of the fiber in use; (b) General sketch of the experimental setup. Voltages and geometry differ among the measurements, crucially, $d_{acc} \ll d_{drift}$.
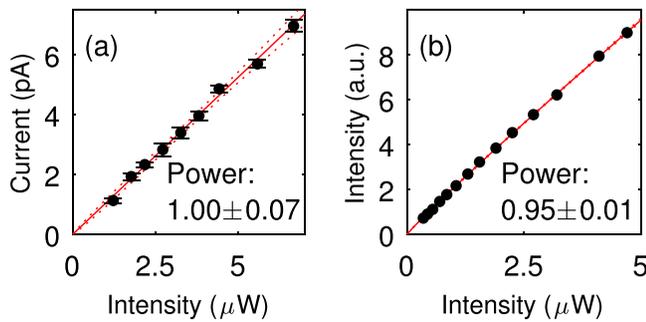
FIG. 2. (a) Measured emitted electron current as a function of the laser power (black squares) and a power-law fit (red line) for the 100 μm fiber; (b) electron beam intensity at the screen position as a function of the laser power (black squares) and a power-law fit (red line) for the 50 μm fiber.

FIG. 3. Measurement results for a 50 μm core size fiber-based cathode. (a) Integrated beam profiles along x as measured on the screen, shown for different positions of the scanning slit (dots), along with fits assuming a homogeneous emission surface (solid lines); (b) intensity profile of the electron beam at the slit along x, determined from the integrated intensity on the screen as a function of slit position. The data points corresponding to the plots in (a) are marked by circles.

At this wavelength, solarization of the fiber through color center formation[17–19] is significant. The 100 μm fiber is a solarization-resistant polyimide coating fiber, while the 50 μm fiber is a standard multi-mode fiber as used in near-field scanning optical microscopy (NSOM) experiments.[20,21] Our optical transmission measurements revealed that a significant fraction of the input laser power is lost in both of the two fibers, with a slightly better transmission for the solarization resistant 100 μm fiber.

The photocathode fiber, coated with 30 nm Au on 3 nm of Cr, was placed inside the vacuum chamber at a base pressure of 5×10^{-9} mbar, and the emission current was measured as a function of the laser power. As shown in Figures 2(a) and 2(b), for both fibers, the emitted current scales linearly with the applied laser power, suggesting single-photon photoemission as being the predominant electron emission mechanism. For the 100 μm fiber, the current was directly measured using an electrometer connected to the photocathode metal; the result is shown in Figure 2(a). An average emission current between 1 and 8 pA was measured, corresponding to 8000 to 44 000 electrons per bunch, and a quantum efficiency (QE) of the Au layer on the order of 10^{-5}, which is in accordance with the values typically reported in the literature. For the 50 μm fiber (Figure 2(b)), the average emission current was too low to be measured directly. Instead, the intensity of the electron beam was measured using a microchannel plate (MCP) detector. The results are shown in Figure 2(b). The main reason for the low emission current is the low laser power that reaches the emitter because of the solarisation of the fiber.

Besides the bunch charge, the main quantity of interest to assess the suitability for next-generation electron diffraction experiments is the transverse emittance, which is conserved along the beam line and defines the coherence length that can be achieved at a given transverse beam size. For this purpose, we used the aperture scan technique, where a 1 μm wide slit aperture (1 mm long) laterally scans the beam along its narrow direction x. The beam width σ_x is measured through the dependence of the transmitted current on the slit position. By observing the image of the transmitted beam on the MCP detector placed in the far field, the angular spread σ_θ at a given slit position can be inferred. Combining both allows to calculate the normalized emittance defined as

$$\epsilon_{rms} = \frac{p_z}{mc} \times \sigma_\theta \sigma_x, \tag{1}$$

where the prefactor comprises the electron momentum along the z-axis p_z as given by the acceleration voltage, the electron mass m, and the speed of light c.

Using this technique, the emittance was measured for each of the two fiber types presented above. For the 50 μm core diameter fiber, the cathode was biased at $V_{acc} = -200$ V, while the slit aperture was grounded and placed 1 mm downstream. The MCP front plate (the detector in Figure 1(b)) situated at a distance d_{drift} of 95 mm away from the fiber was biased at +80 V.

In Figure 3(a), the profile of the beam going through the slit aperture is shown at the screen position for different slit positions. As the slit acts as an imaging pinhole, the peak shape is given by a one-dimensional projection of the homogeneous (top-hat) emission profile (supplementary material, Fig. S1). A corresponding fit is applied, and a local angular spread σ_θ is determined from the RMS width of the beam on the screen when the slit is centered on the intensity peak of the beam. The beam profile at the aperture position is shown in Figure 3(b). It exhibits a Gaussian shape with a RMS width of $\sigma_x = 42$ μm, as determined by applying a Gaussian fit. The resulting normalized emittance for the 50 μm fiber is $\epsilon_{rms} = 4.0$ π nm. This value is on a par with state-of-the-art externally illuminated cathodes[22] and very good when compared to earlier results[23–25] or to the theoretical prediction made by the three-step model for photoemission.[26] The transverse coherence length of the electron bunch at the slit position can be estimated from the measured emittance and beam size using the relation[22,27]

$$L_x = \frac{\hbar}{p_z \sigma_\theta} = \frac{\hbar}{mc} \times \frac{\sigma_x}{\epsilon_{rms}}. \tag{2}$$

Using this equation, we obtain $L_x = 4.1$ nm.

For the $100\,\mu\text{m}$ core diameter fiber, a similar measurement was carried out, at a higher acceleration voltage of $V_{\text{acc}} = -1500\,\text{V}$ and a slightly changed geometry (see the supplementary material for details). Distribution RMS widths of $\sigma_x = 63\,\mu\text{m}$ and $\sigma_\theta = 3.4$ mrad were found, yielding a normalized emittance of $\epsilon_{\text{rms}} = 16.4\,\pi$ nm and a coherence length of $L_x = 1.5$ nm. This larger value was expected, given the larger fiber core size, and hence the emission area. Furthermore, a more inhomogeneous emission pattern was found, assuming a Gaussian instead of top-hat shape led to satisfactory fits (supplementary material, Figure S2).

Finally, we embedded our fiber-based photocathode inside a bulk cathode structure which is optimized for use in high extraction fields as typically employed in compact DC guns (typically in the keV to hundreds of keV regimes[7–9,22,28]) or radio-frequency (RF) guns ranging into MeV energies.[27] The feasibility of this arrangement was tested in a DC electron gun at an acceleration field of 7 MV/m, and beam energy of $70\,\text{kV}$ (see the supplementary material for details). Note that these limits were imposed by the experimental setup used for characterization and are not inherent to our source concept. Photoemission was triggered using a 100 fs pulsed UV (266 nm) laser source at a maximum average input laser power of $400\,\mu\text{W}$. The aperture scan measurements were performed as before, to infer the electron beam emittance. A normalized emittance of $\epsilon_{\text{rms}} = 30.6\,\pi$ nm was obtained, and a mostly uniform emission pattern inferred (supplementary material, Fig. S3). A larger value was expected compared to the low voltage DC gun measurements; the higher acceleration field results in a larger excess energy of emitted electrons due to the Schottky lowering effect, possibly inducing a significant change on the emittance. The increased effects of Coulomb interaction may cause additional growth of the transverse emittance after the emission.

Single-photon ultrafast photoemission was demonstrated for a back-illuminated photocathode based on a coated optical multi-mode fiber. Up to 44 000 electrons were emitted per bunch. Using the aperture scan technique, we have measured beam emittances comparable to what is expected for metal photocathodes at the given spot sizes, which are determined by the fiber core size of our system. Moreover, the feasibility of application to high electric field environments was demonstrated.

See supplementary material for derivation of the data analysis (supplementary Figure S1 and corresponding text) and detailed result plots for the $100\,\mu\text{m}$ fiber (supplementary Figures S2 and S3).

[1]A. H. Zewail, Annu. Rev. Phys. Chem. **57**, 65 (2006).

[2]R. J. D. Miller, Annu. Rev. Phys. Chem. **65**, 583 (2014).

[3]B. J. Siwick, J. R. Dwyer, R. E. Jordan, and R. J. D. Miller, Science **43**, 3 (2003).

[4]A. Janzen, B. Krenzer, O. Heinz, P. Zhou, D. Thien, A. Hanisch, F.-J. Meyer Zu Heringdorf, D. von der Linde, and M. Horn von Hoegen, Rev. Sci. Instrum. **78**, 013906 (2007).

[5]H. Jean-Ruel, M. Gao, M. A. Kochman, C. Lu, L. C. Liu, R. R. Cooney, C. A. Morrison, and R. J. Dwayne Miller, J. Phys. Chem. B **117**, 15894 (2013).

[6]M. Gao, C. Lu, H. Jean-Ruel, L. C. Liu, A. Marx, K. Onda, S.-Y. Koshihara, Y. Nakano, X. Shao, T. Hiramatsu, G. Saito, H. Yamochi, R. R. Cooney, G. Moriena, G. Sciaini, and R. J. D. Miller, Nature **496**, 343 (2013).

[7]M. Hada, D. Zhang, K. Pichugin, J. Hirscht, M. A. Kochman, S. A. Hayes, S. Manz, R. Y. N. Gengler, D. A. Wann, T. Seki, G. Moriena, C. A. Morrison, J. Matsuo, G. Sciaini, and R. J. D. Miller, Nat. Commun. **5**, 3863 (2014).

[8]T. Ishikawa, S. A. Hayes, S. Keskin, G. Corthey, M. Hada, K. Pichugin, A. Marx, J. Hirscht, K. Shionuma, K. Onda, Y. Okimoto, S.-y. Koshihara, T. Yamamoto, H. Cui, M. Nomura, Y. Oshima, M. Abdel-Jawad, R. Kato, and R. J. D. Miller, Science **350**, 1501 (2015).

[9]L. Waldecker, T. A. Miller, M. Rudé, R. Bertoni, J. Osmond, V. Pruneri, R. E. Simpson, R. Ernstorfer, and S. Wall, Nat. Mater. **14**, 991 (2015).

[10]M. Schmitt, "Feldunterstutzte Photoelektronenemission," Ph.D. thesis, University of Darmstadt, 1998.

[11]T. Vecchione, U. Weierstall, C. Edgcombe, and J. Spence, Microsc. Microanal. **12**, 146 (2006).

[12]J. Spence, T. Vecchione, and U. Weierstall, Philos. Mag. **90**, 4691 (2010).

[13]D. R. Turner, U.S. patent 4469554 (1984).

[14]R. Kazinczi, E. Szocs, E. Kalman, and P. Nagy, Appl. Phys. A **66**, S535 (1998).

[15]P. Uebel, S. T. Bauerschmidt, M. A. Schmidt, and P. St. J. Russell, Appl. Phys. Lett. **103**, 021101 (2013).

[16]A. Casandruc, G. Kassier, H. Zia, R. Bücker, and R. J. D. Miller, J. Vac. Sci. Technol., B: Nanotechnol. Microelectron.: Mater., Process., Meas., Phenom. **33**, 03C101 (2015).

[17]P. Karlitschek, G. Hillrichs, and K. Klein, Opt. Commun. **155**, 376 (1998); **155**, 386 (1998).

[18]L. Skuja, H. Hosoflo, M. Hiranob, and S. Si, Proc. SPIE **4347**, 155–168 (2001).

[19]K.-F. Klein, C. P. Gonschior, D. Beer, H.-S. Eckhardt, M. Belz, J. Shannon, V. Khalilov, M. Klein, and C. Jakob, Proc. SPIE **8775**, 87750B (2013).

[20]B. Hecht, B. Sick, U. P. Wild, V. Deckert, R. Zenobi, O. J. F. Martin, and D. W. Pohl, J. Chem. Phys. **112**, 7761 (2000).

[21]L. Lereu, A. Passian, and P. Dumas, Int. J. Nanotechnol. **9**, 488 (2012).

[22]C. Gerbig, A. Senftleben, S. Morgenstern, C. Sarpe, and T. Baumert, New J. Phys. **17**, 043050 (2015).

[23]S. D. Moustaizis, M. Tatarakis, C. Kalpouzos, and C. Fotakis, Appl. Phys. Lett. **60**, 1939 (1992).

[24]K. L. Jensen, W. Dc, D. W. Feldman, E. J. Montgomery, P. G. O. Shea, C. Park, N. A. Moody, L. Alamos, J. Petillo, and Science Applications International Corporation, in *Proceedings of PAC07, New Mexico* (2007), p. 1377.

[25]H. Kassier, "Ultrafast electron diffraction: source development, diffractometer design and pulse characterisation," Ph.D. thesis, University of Stellenbosch, 2010.

[26]D. Dowell, P. Bolton, J. Clendenin, P. Emma, S. Gierman, W. Graves, C. Limborg, B. Murphy, and J. Schmerge, Nucl. Instrum. Methods Phys. Res. Sect., A **507**, 327 (2003); D. H. Dowell, F. K. King, R. E. Kirby, and J. F. Schmerge, Phys. Rev. Spec. Top. - Accel. Beams **9**, 063502 (2006); D. H. Dowell and J. F. Schmerge, *ibid.*. **12**, 074201 (2009).

[27]S. Manz, A. Casandruc, D. Zhang, Y. Zhong, R. A. Loch, A. Marx, T. Hasegawa, L. C. Liu, S. Bayesteh, H. Delsim-Hashemi, M. Hoffmann, M. Felber, M. Hachmann, F. Mayet, J. Hirscht, S. Keskin, M. Hada, S. W. Epp, K. Fï Ottmann, and R. J. D. Miller, Faraday Discuss. **177**, 467 (2015).

[28]D. S. Badali, R. Y. N. Gengler, and R. J. D. Miller, Struct. Dyn. **3**, 034302 (2016).